



Publisher homepage: www.universepg.com, ISSN: 2663-7804 (Online) & 2663-7790 (Print)

<https://doi.org/10.34104/ajeit.024.037050>

Australian Journal of Engineering and Innovative Technology

Journal homepage: www.universepg.com/journal/ajeit

Australian Journal of
Engineering and
Innovative Technology



UNIVERSE PUBLISHING GROUP
www.universepg.com

Analyzing Flood Damage and Mapping Flood Hazard Zones Using AHP Model: A Case Study of Pol-e-Alam, Logar Province, Afghanistan

Karimullah Ahmadi^{1,2*}, Ahmad Shakib Sahak^{3,4}, Abdul Basir Azizi^{5,6}, Mohammad Anwar Saraj⁷, and Ahmad Tamim Sahak⁶

¹Dept. of Aerospace Research of the Earth, Photogrammetry, Moscow State University of Geodesy and Cartography, Moscow, Russian Federation; ²Dept. of Civil Engineering, Nangarhar University, Jalalabad, Afghanistan; ³Dept. of Remote Sensing and Photogrammetry, Karadeniz Technical University, Trabzon, Türkiye; ⁴Dept. of Geographical Information System Kabul Polytechnic University, Kabul, Afghanistan; ⁵Dept. of Cadaster and Monitoring, State University of Land Use Planning, Moscow, Russia; ⁶Dept. of Engineering Geodesy Kabul Polytechnic University, Kabul, Afghanistan; and ⁷Faculty of Geomatics and Cadaster, Dept. of Engineering Geodesy, Kabul Polytechnic University, Kabul, Afghanistan.

*Correspondence: ahmadi.niazai33@gmail.com (Karimullah Ahmadi, Assistant Professor, Dept. of Civil Engineering, Nangarhar University, Jalalabad, Afghanistan).

ABSTRACT

This research aims to evaluate the impact of the most recent floods that occurred on August 20, 2022, in Logar province in southern Afghanistan. For this purpose, changes in land use and land cover (LULC) of the study area were created from the Sentinel-2 image with a spatial resolution of 10 meters. To achieve this, the study utilized Sentinel-2 images to analyze LULC changes before and after the flood event and employed a support vector machine for supervised classification. The study also applied the analytical hierarchy process (AHP) to evaluate the future risks of flooding in the study area, focusing on factors related to hydrological phenomena. Overall, the study demonstrates the effectiveness of geospatial technologies and remote sensing in assessing the impacts of floods and creating flood risk maps. This can significantly reduce the consequences of flooding and inform decision-making for disaster management and mitigation.

Keywords: Flood, Remote sensing, Senteinel-2, SNAP, AHP, GIS, and Multi-criteria decision making.

INTRODUCTION:

Flooding is one of the most common and destructive natural hazards, endangering lives and the economy (Khan *et al.*, 2011). Floods are becoming more intense due to human activities that lead to land use change and climate change (Khan *et al.*, 2011). Floods are natural hazards that are inevitable and are expected to be more severe in the future (Allafta & Opp, 2021). Therefore, current pattern and future flood hazard scenarios require accurate spatial and temporal inform-

ation on the potential flood hazards (Ouma & Tateishi, 2014). Flood is defined as a flow of water that inundates higher ground under abnormal conditions or at a level above the typical water surface (Rahman, 2006). It is a common natural disaster brought on by excessive rain that destroys property, claims lives, and destroys a large area of agricultural and plants. In general, disaster management can be divided into three phases: preparatory, which involves identifying threat zones before a disaster; mitigation, which involves

conducting emergency evacuation, tracking, and executing contingency plans beforehand or during a disaster; and response, which involves assessing damage and implementing recovery measures soon afterwards (Jeyaseelan, 2003). Recent advancements in space technology allow researchers and agencies to use satellite images. Flooding period and extent may also be roughly determined by these images (Veljanovski *et al.*, 2011), and mapping flooded areas is a crucial step in understanding the altered land use and land cover (D'Addabbo *et al.*, 2018). Thus, evaluating flood risks and adopting appropriate management and mitigation strategies can significantly reduce related risks (Allafta & Opp, 2021; Le Bihan *et al.*, 2017). Determining flood risk areas and applying appropriate mitigation measures can significantly reduce flood damage (Le Bihan *et al.*, 2017; Naulin *et al.*, 2013). In addition, flood risk mapping plays a significant role in land use management, early warning systems, emergency response design and flood risk mitigation estimations (Allafta & Opp, 2021; Zhang & Chen, 2019). Central Asian countries, including Afghanistan, Kazakhstan, Uzbekistan, Turkmenistan, Tajikistan, and Kyrgyzstan, are considered to have extremely continental climates (Gerlitz *et al.*, 2018; Sahak *et al.*, 2023). They are typically counted as arid and semi-arid regions due to less rainfall during the summer season compared to North and South Asian countries (Gerlitz *et al.*, 2018).

Afghanistan experiences hot summers and cold winters, with the lowest annual precipitation of about 30 mm in the southwest and the highest precipitation exceeding 100 mm in the northeast (Sahak *et al.*, 2023; Nur *et al.*, 2021). According to officials, intense rainfall from August 20th to 23rd, 2022, led to flash floods in Logar, an eastern province of Afghanistan, resulting in the deaths of over twenty individuals and the destruction of over 3000 residences. Additionally, numerous canals were ruined, approximately 5000 acres of agricultural land, primarily orchards, were devastated, and around 2000 livestock perished (ARAB, 2022). Logar Province, due to its location and the fact that most of its residential settlements and agricultural lands are close to the river and its low elevation, is prone to flooding. Among the most affected areas was Pol-e-Alam District of this province, which

was completely submerged. Flood risk evaluation using numerical models is a common method for flood hazard estimation (Vu *et al.*, 2015). Hydrological and hydrodynamic models are widely used to evaluate floods according to their magnitude, extent, and frequency (Aribisala *et al.*, 2022). The runoff efficiency model, another hydraulic method, mainly examines flood routing issues in waterways (Dilley, 2005; Khan *et al.*, 2011). These quantitative models can evaluate various datasets and offer important insights on the potential for flooding (Wang *et al.*, 2011). However, the most prevalent and challenging issue with such a system is the lack of hydro-meteorological data (Cabrera & Lee, 2019). Many researches have utilized GIS-based multi-criteria evaluation analysis (MCEA) to assess flood risk by investigating the role of factors that control floods (Allafta & Opp, 2021; Desalegn & Mulu, 2021; Hasanloo *et al.*, 2019; Saha & Agrawal, 2020; Tavus *et al.*, 2022). The GIS-MCEA approach utilizes the advantage of GIS for spatial data processing and the adaptability of MCDA to integrate factual data, such as rainfall, land use, slope, soil, and drainage density, with weights-based data (Adesina *et al.*; Stefanidis & Stathis, 2013; Yahaya *et al.*, 2010). GIS-based MCEA explores complicated decision-making problems by hierarchically stacking control factors (Chen *et al.*, 2011). The model is experts' knowledge-based and was first introduced by Saaty (Razandi *et al.*, 2015a; Saaty, 1980). AHP is an essential way to compute the weights of each parameter for achieving the goal in the decision-making of complex problems (Ahmadi *et al.*, 2020). Comparing the influencing parameters based on their relative importance to the target decision by a pairwise comparison matrix is considered the early stage of the AHP model (Ghosh *et al.*, 2020; Şener *et al.*, 2018a). In numerous studies focused on natural hazard assessment, researchers have shown that integrating GIS and AHP within an MCEA framework has proven to be effective, particularly in the context of flood hazard mapping (Feizizadeh, 2013), groundwater potential zoning mapping (Arshad *et al.*, 2020), and soil erosion susceptibility mapping (Kachouri *et al.*, 2014). The efficiency of such a method (i.e. combination of GIS with AHP in the MCEA paradigm) in hazard mapping is significantly due to its capacity to deal with data scarcity (Cabrera & Lee,

2019). In this study, the most common factors used in flood risk mapping were slope, digital elevation model (DEM), drainage density, LU/LC, NDVI, and distance from rivers (**Table 2**). Variables are often chosen according to a comprehensive review of the literature, and their weights are assigned based on expert knowledge using the AHP approach (Adesina *et al.*; Allafta & Opp, 2021; Cabrera & Lee, 2019; Hasanloo *et al.*, 2019; Rahman, 2006; Stefanidis & Stathis, 2013; Yahaya *et al.*, 2010). This research attempted to evaluate the areas affected by flooding pre- and post-flood, and also applied the Analytical Hierarchy Process (AHP) algorithm to evaluate the flood risk assessment zone in Logar, Pol-e-Alam district, Afghanistan. This is the first study to be conducted in the Pol-e-Alam district, and is based on a spatial analysis carried out using the AHP model and taking the most relevant factors influencing natural hazards into account. The novelty of the methodology and the outcomes of this study will scientifically assist the managers and policy makers of the Office of State Minister for Disaster Management of Afghanistan, and other involved national and inter-national organizations with a more comprehensive analysis and clear instructions for creating early warning systems, emergency response processes, flood risk mitigation estimations, and suggesting where future development

should be avoided or restricted. Consequently, the objectives of this study are as follows:

- a) Estimating land use and land cover using sentinel-2 satellite imagery.
- b) Evaluation of flood affected map using land use and land cover map.
- c) Utilizing the analytical hierarchy process (AHP) to analyze and produce a flood risk assessment map.

MATERIALS AND METHODS:

Study area Pol-e-Alam district is the capital of Logar province in Afghanistan (**Fig. 1**). Logar is generally described as a relatively flat river valley in the north and central zones. The east, south and southwest of Logar province is surrounded by rugged mountains. The Logar province is located at an elevation of 2186 meters above sea level; it has a humid, continental, and warm summer climate. The population of Logar was 121,935 in 2021. The average annual temperature is 11.4°C (52.52°F), which is 4.3% lower than Afghanistan's norms. The climate in the area is extremely conducive to agriculture and varies according to elevation. The average annual rainfall in Logar is roughly 32.07 millimeters, and there are 81 wet days per year (Nasimi *et al.*, 2020).

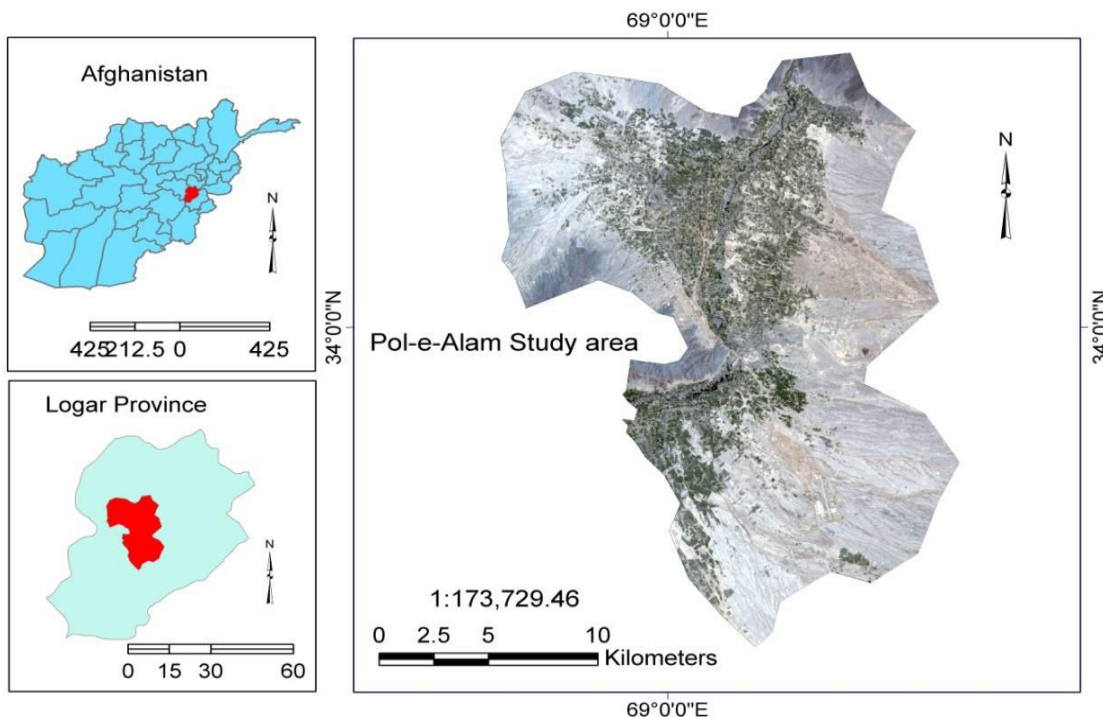


Fig. 1: Location of study area.

Dataset

In this study, Sentinel-2 imagery for the study area is acquired from the Copernic website. Images are chosen for two distinct times, pre-flood and post-flood, with dates of August 12, 2022, and August 28, 2022, respectively. To map the flood-affected areas, Sentinel-2 images were chosen based on these dates. Two images' tiles were used to cover the study area. To obtain the image of the Pol-e-Alam district, both image tiles are mosaicked and stacked for each date. Digital Elevation Model was downloaded from the USGS Earth Explorer website (<https://earthexplorer.usgs.gov/>). Two tiles of elevation images that are compatible with the research region were downloaded and mosaicked. In order to calculate flood risk assess-

ment map using AHP algorithm, various thematic maps (slope, drainage density, lulc, elevation, distance from river, and NDVI) are created.

Methodology

The general methodology followed for this study is represented in (Fig. 2). Sentinel-2 imagery is utilized to identify the areas that have been flooded during 2022. A flood affected map is created based on this information. Then the area of each LULC class that was affected by the flood is determined. Finally, the AHP technique is utilized to map the flood risk assessment for the entire research area. The next sections provide a thorough description, step by step, of each part of these methodologies.

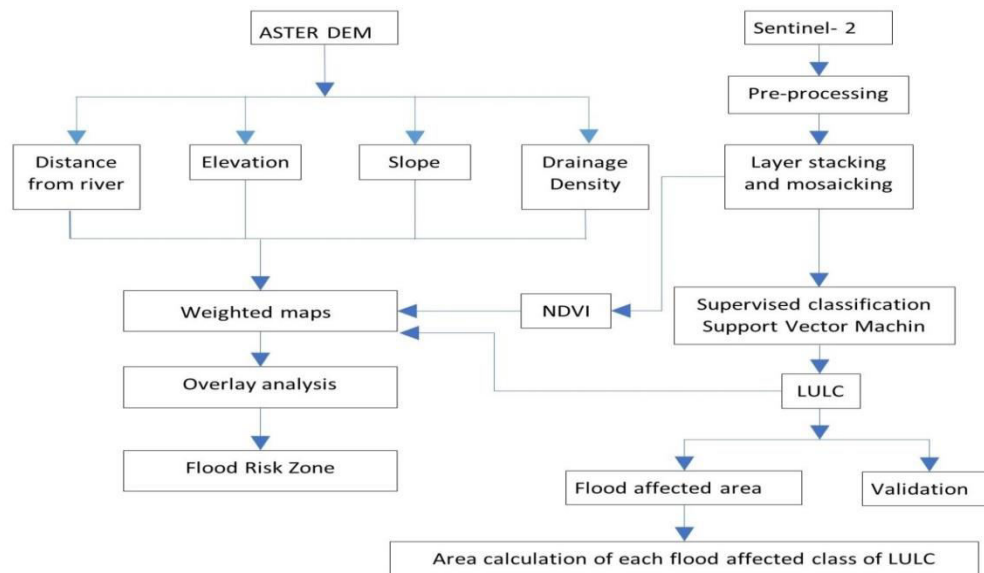


Fig. 2: Methodological scheme.

Assessment of flood-affected land cover classes

In order to calculate and evaluate the flood-affected land cover types, Sentinel-2 images from August 12, 2022, pre-flood, and August 28, 2022, post-flood, are used. The study area is covered by two tiles of image, so the images are mosaicked, the study area is clipped based on the shape file of the study area, the preprocessing of the image is done in SNAP, and then supervised classification of Sentinel-2 images of the before and after flood is done to produce the land use

and land cover map. As a supervised classification technique, the support vector machine algorithm has been utilized. The LULC map is classified into four categories: agriculture, built-up areas, barren areas, and water (Fig. 3). To identify the water and non-water areas, each classified image is reclassified, and finally, it is determined how much of each LULC class is affected by the flood as demonstrated in (Fig. 4) and (Table 1).

Table 1: Analysis of Land Use and Land Cover Change for pre-flood and post-flood.

Time	Agriculture km2	Built up km2	Barren area km2	Water km2	Total area km2
Pre - Flood	149.68	23.33	195.90	5.63	374.31
Post - Flood	139.32	22.71	195.59	16.69	374.31

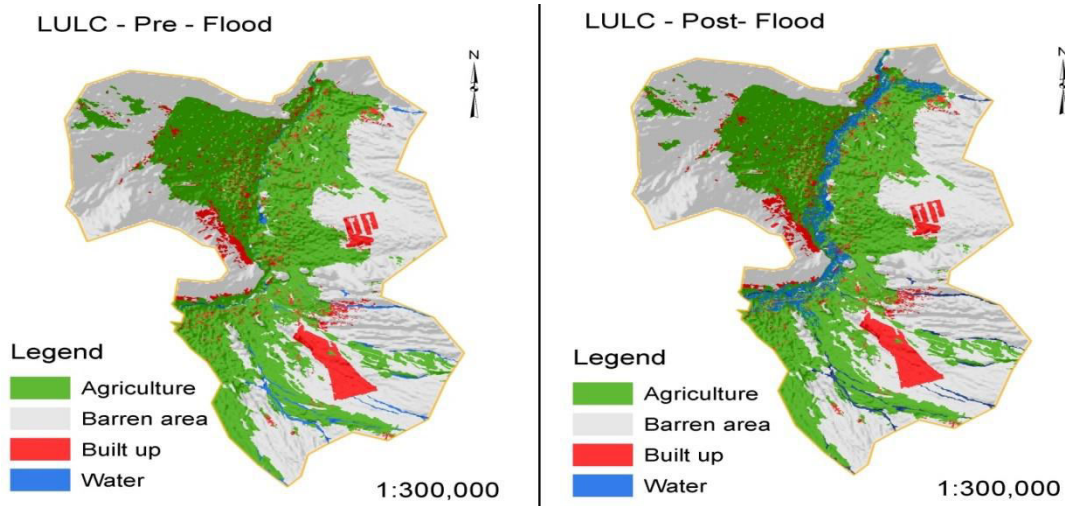


Fig. 3: Land use and Land cover pre - flood and post - flood, using sentinel-2.

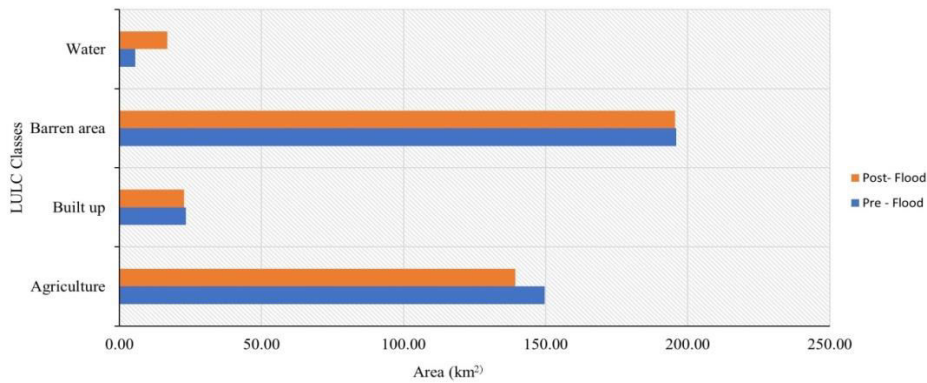


Fig. 4: Change detection of land use/land cover in the study area pre - flood and post - flood.

The land use change pattern in the study area is consistent with the classification result of Sentinel-2 image. The pre-flood image makes agriculture and built-up areas along the river very evident (**Fig. 5a**).

On the other hand, the post-flood image (**Fig. 5b**) exhibits an abnormal change in water area that expanded sharply and resulted in flooding of all nearby built-up and agricultural areas.

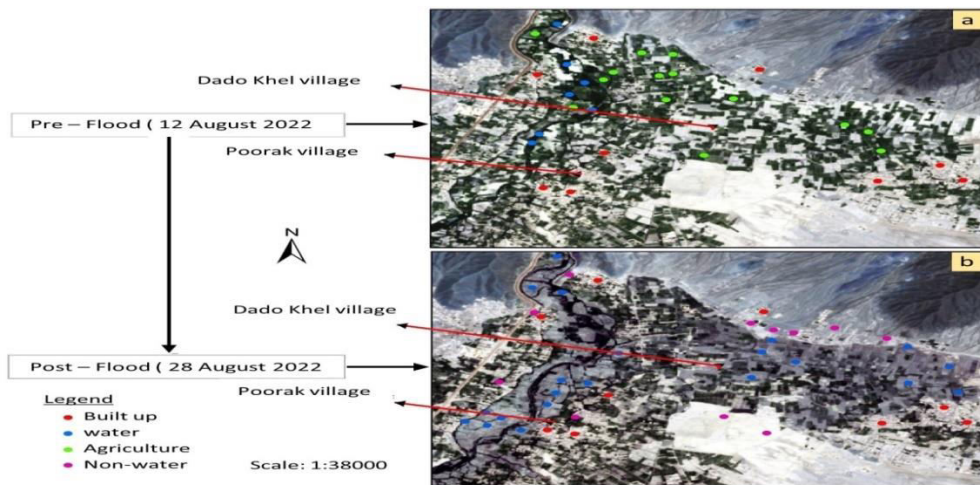


Fig. 5: (a) - Sentinel-2 image Pre-flood, 12 August, 2022, and (b) - post-flood, 28 August, 2022, are shown some of the validation points.

AHP Technique for Evaluating the Flood Risk Assessment

AHP is a critical method for calculating the weights of each factor in the decision of complex problems (Ahmadi *et al.*, 2022). The approach relies on expert knowledge and was initially developed by Saaty (Razandi *et al.*, 2015b; Saaty, 1990). The initial step in the AHP model involves creating a matrix for pairwise comparisons of influencing factors and their respective significance in the decision-making process (Şener *et al.*, 2018b). The normalized weights calculation, consistency ratio calculation, and ultimate decision of making steps are the other phases of this model. In this study, six factors (elevation, drainage density, slope, land use and land cover, distance from the river, and NDVI) associated with hydrological processes are evaluated using the Saaty, (1977) scale ranging from 1 (equal importance) to 9 (very high importance). These factors are compared in pairs to create a matrix, as illustrated in (Table 2). Elevation: is considered as one of the key causes of flooding (Seejata *et al.*, 2018). Flood risk is inversely related to elevation since lower elevations are more susceptible to floods than higher elevations (Tang *et al.*, 2018). The depth, direction, and extent of the flood are significantly influenced by elevation. Digital Elevation Model (DEM) serves as the elevation layer. In this study, the study area is divided into five categories: very low, low, medium, high, and very high, with respective ranges of 1868 - 1929, 1929 - 1981, 1981 - 2041 - 2041 - 2113 and 2113 - 2264 meters. Drainage density: is still another crucial factor of flood risk, that the chances of higher flood occurrence are associated with higher runoff, which is directly related to the higher value of drainage density (Mahmoud & Gan, 2018). The greater drainage density is a favorable indicator that the basin has a higher flow accumulation channel. A higher streamline density suggests a greater amount of excess

runoff and, consequently, a higher risk of floods. The stream polyline feature is created for the drainage density layer. After the drainage density layer is formed, it is divided into five classes: 0 - 128, 128 - 276, 276 - 423, 423 - 619, and 619 - 1018. The higher chance of water accumulated is related to the higher range of drainage density. Slope: Floods are more likely to occur in flat or low-sloped locations (Seejata *et al.*, 2018). Slope is directly associated with runoff velocity and vertical percolation. Slope and stream power are directly correlated in the downstream. The slope is measured in degrees and divided into five groups, ranging from 0° - 2°, 2° - 4°, 8° - 16°, and 16° - 34°. LULC and NDVI: The infiltration rate is directly affected by LULC and NDVI. In comparison to urban areas, the vegetated areas can accommodate more infiltration (Seejata *et al.*, 2018). Flooding frequency can be significantly influenced by land use patterns (Das, 2019). Urbanized and developed surfaces produce greater runoff, which is much more stubborn to subside with time. As a result, urbanized areas and developed shorelines are more flood-prone than bare soil and vegetated land covers. As previously stated, the identified parameters were grouped into six categories and assigned rankings based on their relative significance within each subcategory, as demonstrated in (Table 2). The significance of each category and subcategory was derived from existing literature and understood in terms of their implications for flood risk assessment. In order to generate the flood risk map, six important hydrological phenomena parameter layers are created. Then, the criteria classes are reclassified in order to provide weight. Each parameter's weight is shown in (Table 5), in a hierarchical order. Multi-criteria decision-making is used to create the flood risk map. As a tool for multi-criteria decision-making, the AHP technique has been employed.

Table 2: Flood Susceptibility Criteria and sub - criteria Ranges for Flood Susceptibility Assessment.

Flood Causative Criterion	Unit	Classes	Susceptibility Class Ranges and Ratings	Susceptibility Class Ratings
Slope	Degree	0 – 2	Very High	5
		2 – 4	High	4
		4 – 8	Moderate	3
		8 – 16	Low	2
		16 – 34	Very Low	1
Drainage	Level	0 – 128	Very Low	1

Density		128 – 276	Low	2
		276 – 423	Moderate	3
		423 – 619	High	4
		619 – 1018	Very High	5
	LULC	Level	Water	Very High
		Agriculture	High	4
		Built up	Moderate	3
		Barren area	Low	2
Elevation	m	1868 – 1929	Very High	5
		1929 – 1981	High	4
		1981 – 2041	Moderate	3
		2041 – 2113	Low	2
		2113 – 2264	Very Low	1
Distance from River	m	0 – 596	Very High	5
		596 – 1400	High	4
		1400 – 2463	Moderate	3
		2463 – 4097	Low	2
		4097 – 6612	Very Low	1
NDVI	Level	-0.23 – 0.05	Very High	5
		0.05 – 0.11	High	4
		0.11 – 0.21	Moderate	3
		0.21 – 0.32	Low	2
		0.32 – 0.60	Very Low	1

Pairwise comparison the factors

The Saaty, (1980) comparative scale is one of the most common methods for comparison. Considering this method, a comparative scale is made up of integers from 1 to 9. As a result, the number one represents the least important factor, while the number nine represents the most important factor. The comparison process was done for all six factors, and the relative

weight of each factor was evaluated (Table 3). Furthermore, the normalized matrix and weight for each parameter were calculated, as shown in (Table 4, 5). To examine the discrepancy between pairwise comparisons and the reliability of the obtained weights, the consistency ratio (CR) should be calculated.

Table 3: Pairwise comparison matrixes.

	Slope	Drainage	Elevation	LULC	NDVI	Distance from river
Slope	1.00	2.00	3.00	4.00	6.00	9.00
Drainage	0.50	1.00	2.00	3.00	5.00	8.00
Elevation	0.33	0.50	1.00	2.00	4.00	6.00
LULC	0.25	0.33	0.50	1.00	3.00	4.00
NDVI	0.17	0.20	0.25	0.33	1.00	2.00
Distance from river	0.11	0.13	0.17	0.25	0.50	1.00

Table 4: Normalized Pairwise matrix calculated.

	Slope	Drainage density	Elevation	LULC	NDVI	Distance from river
Slope	0.42	0.48	0.43	0.38	0.31	0.30
Drainage	0.21	0.24	0.29	0.28	0.26	0.27
Elevation	0.14	0.12	0.14	0.19	0.21	0.20
LULC	0.11	0.08	0.07	0.09	0.15	0.13
NDVI	0.07	0.05	0.04	0.03	0.05	0.07
Distance from river	0.05	0.03	0.02	0.02	0.03	0.03

Table 5: Weighted of each parameter.

Flood Factors	Criteria weighted	Criteria Normalized weighted	Influence (%)
Slope	0.39	2.32	38
Drainage	0.26	1.55	27
Elevation	0.17	1.00	17
LULC	0.11	0.64	11
NDVI	0.05	0.30	5
Distance from river	0.03	0.18	3

In AHP, consistency is used to construct a matrix and is expressed by a consistency ratio that must be < 0.1 to be accepted. Otherwise, the subjective judgments (Saaty & Vargas, 2001) need to be revised and recalculated. The following formula is used to calculate the consistency ratio (CR):

$$CR = \frac{CI}{RI} \dots\dots\dots(1)$$

Where IR is the random inconsistency, which was standard using Saaty, (1980) and the value depends on the number of aspects (n); in this study, there are six factors denoted as n = 6, with a consistency index (CI) calculated using equation 2 and a random index (RI) value of 1.24.

$$CI = \frac{\lambda - n}{n - 1} \dots\dots\dots(2)$$

Where n is the number of elements and λ is the consistency vector's average value. Furthermore, a weighted overlay analysis was performed to create a flood risk assessment map. The Flood Risk Index (FRI) layer is calculated using equation 3.

$$FRI = \sum_{i=1}^n P_i W_i \dots\dots\dots(3)$$

Where W is the weight of factors i and P is the rating of an individual parameter, moreover, the values that were derived from the FRI index were grouped into four hazard classes according to the probability of flood occurrence. This classification was done using multi-criteria decision analysis with the help of the spatial analyst tool in ArcGIS.

RESULTS AND DISCUSSION:

Assessment of flood affected area

Table 6: Flood-affected areas within each LULC.

Time	Agriculture km ²	Built up km ²	Barren area km ²	Water km ²	Total area km ²
Pre - Flood	10.36	0.67	0.31	0.54	11.88

The land use and land cover map was developed to assess the impact of flooding on the area's land use and cover. In this research, the support vector machine supervised classification algorithm was employed to categorize the study region into four main types: agriculture, urban areas, barren land, and water bodies. By reclassifying the LULC map into "water" and "non-water," classes, the flood-affected map was generated, the outputs, indicate that 11.88 km² were affected by the flood. Additionally, the area of each class of land use that is affected by flood is calculated, and the results are presented as a statistical graph and tabulation (**Fig. 6, 7, 8**). The majority of the flood-affected area is located close to the Logar main river. It is evident from the map of the flood-affected land use and land cover that the agricultural area is severely affected by flooding; 10.36 km² of agricultural land has been affected, resulting in loss of people's lands and agricultural products. The majority of the affected agricultural area is situated on both sides of the Logar River. While 0.67 km² of built-up area has been affected by flooding, resulting in the loss of both property and lives, 0.31 km² of barren area has also been impacted by the floods. (**Table 6**) shows the area of each land use and land cover class that was impacted by the flood. As it was shown, flooding is a frequent occurrence in the floodplains close to the Logar River. As there are no significant water bodies or river channels close to the affected areas, the north-eastern section of the research area has only experienced minor flooding as a result of rainfall. The sections on either side of the river that were inundated were primarily caused by the accumulation of excess water during the summer rainfall.

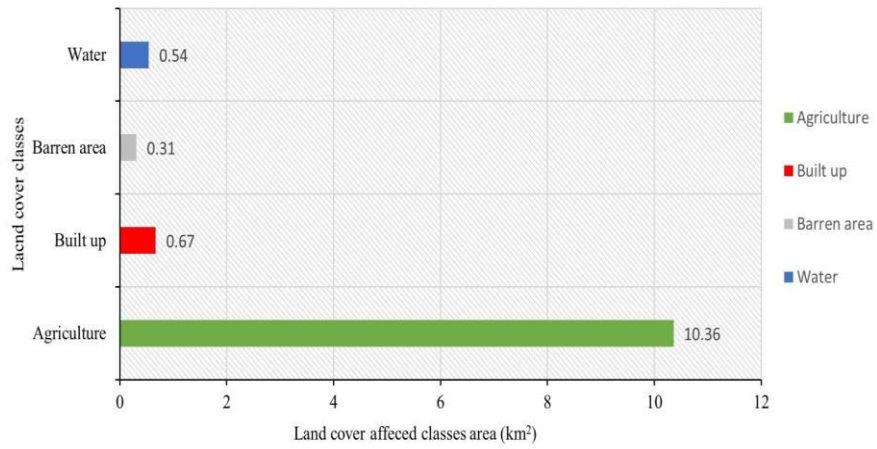


Fig. 6: Statistically analysis flood affected classes of land use and land cover.

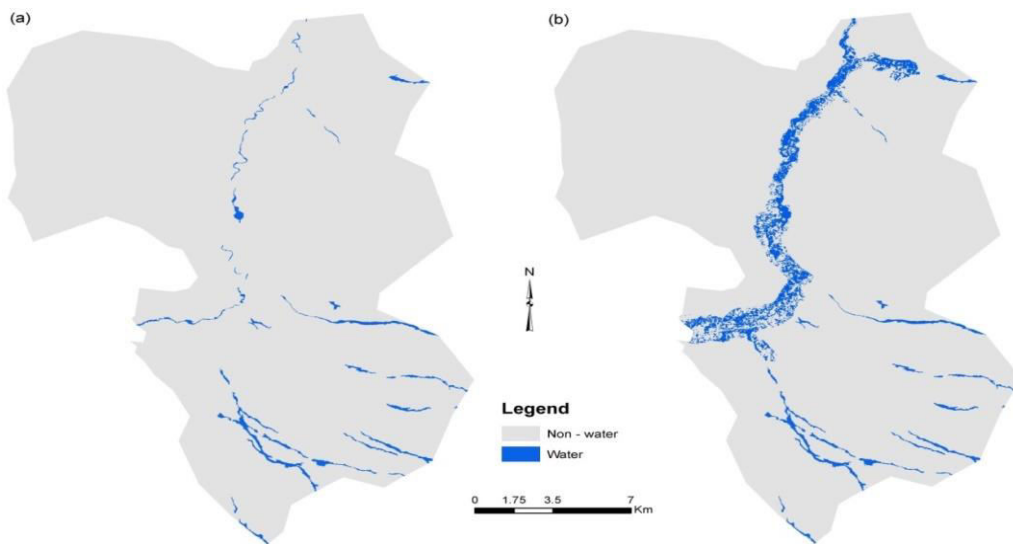


Fig. 7: LULC of the study area into water and non-water classes.

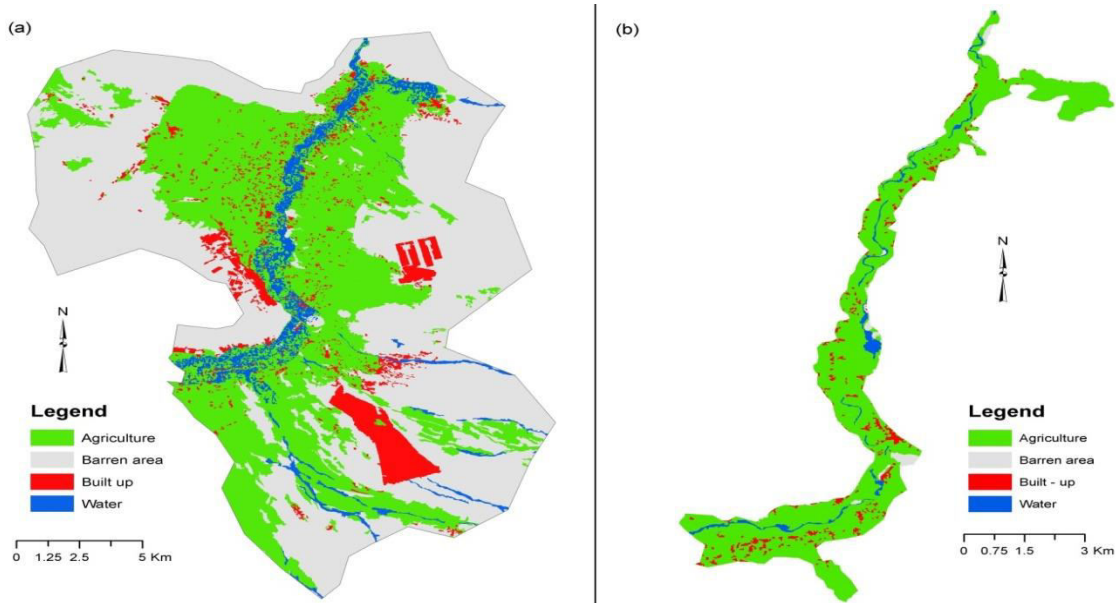


Fig. 8: Flood affected classes of land use and land cover.

Flood Risk Assessment AHP

The AHP technique was used for the weighted classified flood-generating components, and a pair-wise comparison was performed on a 9-point significance scale for all six factors. Based on Saaty's, (1980) suggestion, weighting methods were utilized to prioritize the relative importance of individual factors in a weighted overlay compared to other factors. The six parameters that are considered to have the most impact on the flood risk is elevation, slope, drainage density, NDVI, distance from a river, and land use and land cover. These criteria have already been explained in detail. We generated weighted maps for these parameters using ENVI, SNAP, and ArcGIS software, and the maps for six parameters are shown in (Fig. 9). Based on the results of the flood risk assessment map, the

study area was divided into four zones of flood occurrence: high risk, moderate risk, low risk, and very low risk (Fig. 10, 11). The possibility of flooding on both sides of the Logar River can be well seen. Flooding is more likely in areas near the river and at low elevations. A significant portion of the studied area is under high and moderate risk, due to its proximity to the Logar River, so that the entire study area from Niazi Khel village to Shahghashi village on both sides of the river is under high risk of flooding; respectively, 15.10 km² are under high risk and 179.50 km² are under moderate flood risk. Furthermore, based on the Fig. 9, the outputs reveal, that the majority of the villages, which are closer to either side of the river are in a moderate flood zone.

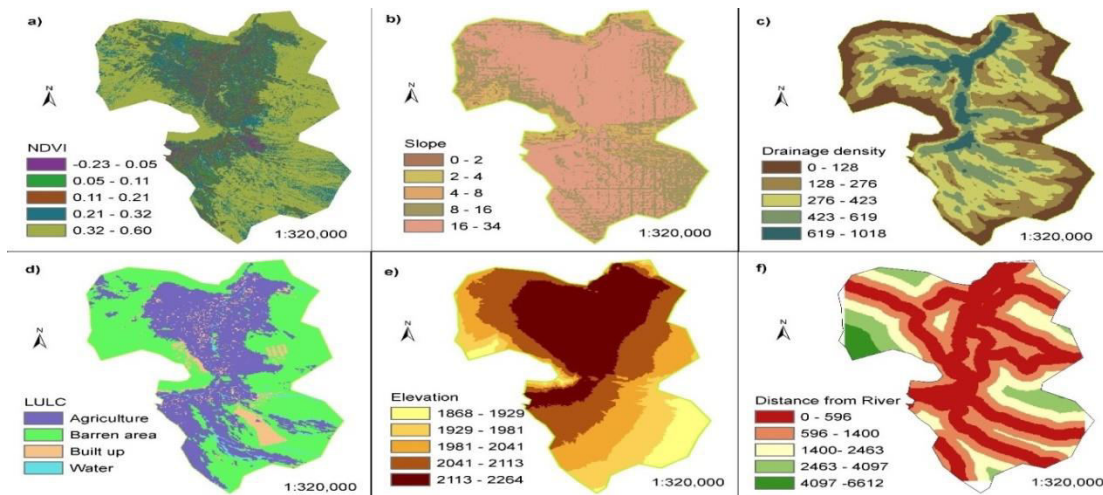


Fig. 9: Flood vulnerability factors maps.

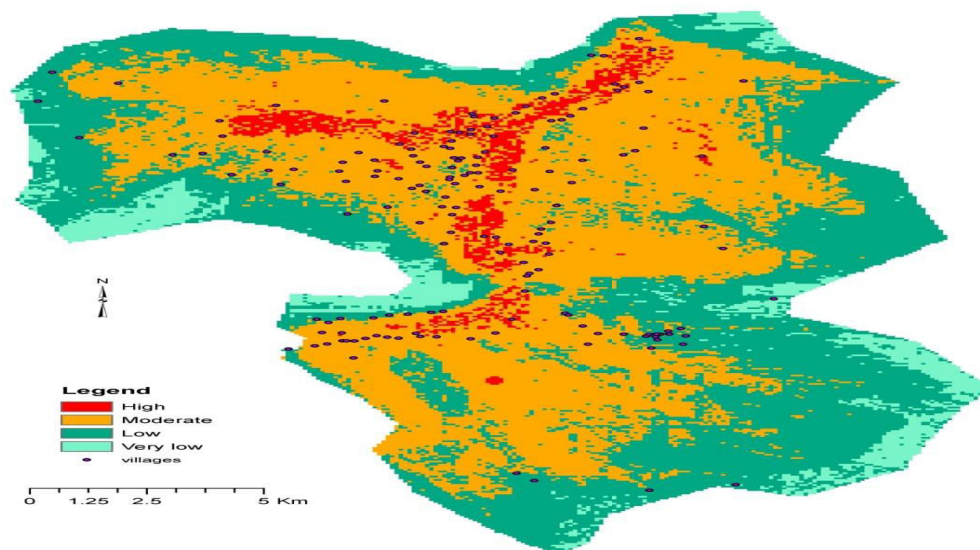


Fig. 10: Flood Risk Assessment Map.

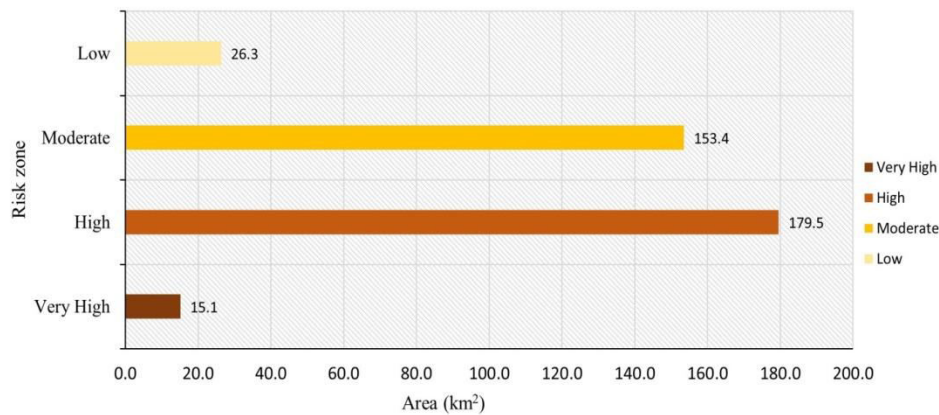


Fig. 11: The graph shows the flood risk zones.

Consequently, based on the out-comes of this study, it will scientifically assist the managers and policy makers of the Office of State Minister for Disaster Management of Afghanistan, and other involved national and international organizations with a more comprehensive analysis and clear instructions for creating early warning systems, emergency response processes, flood risk mitigation estimations, and suggesting where future development should be avoided or restricted.

CONCLUSION:

Remote sensing has the benefit of synchronized and cost-effective data for monitoring flood impacts and risks, as well as their environmental effects on local, regional, and global scales. This research evaluated the impacts and risks of the flood that occurred on August 20, 2022, in the Logar province of Afghanistan. For this, the flood-affected area was calculated through the Sentinel-2 satellite images. The study area was classified into four classes using support vector machine supervised classification algorithm pre- and post-flooding (built-up area, agriculture, barren area, and water). Then, the classified maps were reclassified into "water" and "non-water," classes, the flood-affected area was determined. Based on the results, 11.88 km² of the study area was inundated. And also, according to land use and land cover maps, the outputs showed, that the flood-submerged areas of the different land use and land cover classes (agriculture, built-up areas, and barren) are respectively as follows: 10.37 km², 0.67 km², and 0.3 km². The AHP approach was used to prepare the flood risk map. Therefore, the flood risk parameters or criteria were first identified, and then

the AHP was performed. Then, through the weighted overlay analysis, a flood risk map was generated. From the generated flood risk map the study area was divided into four zones: high, moderate, low, and very low. Based on the outputs of the flood risk map, it was revealed that the Niazi Khel and Shahghashi villages on both sides of the river are at high risk of flooding. The outputs of risk map generated based on AHP algorithm also confirmed that, the highly flood affected areas are generally located near the Logar river. Consequently, based on the above outputs, policy-makers in the Office of State Minister for Disaster Management of Afghanistan, and other involved national and international organizations should be concerned with a more comprehensive analysis and clear instructions for creating early warning systems, emergency response processes, flood risk mitigation estimations, and suggesting where future development should be avoided or restricted.

ACKNOWLEDGEMENT:

I would like to thank our colleagues for their assistance and guidance in helping us successfully complete this work.

CONFLICTS OF INTEREST:

The authors declare that there is no conflict of interest to publish it.

REFERENCES:

- 1) Adesina, E., Adewuyi, A., & Nioku, D. Geomorphic Assessment of Flood Hazard within the Urban Area of Chanchaga Local Government Area, Minna, Nigeria. *Inter J. of Environment and Geoinformatics*, 9(1), 102-115.

- 2) Ahmadi, H., Kaya, O. A., & Pekkan, E. (2020). GIS-based groundwater potentiality mapping using AHP and FR models in central antalya, Turkey. *Environmental Sciences Proceedings*, **5**(1), 11.
- 3) Ahmadi, H., Sahak, A. S., & Karsli, F. (2022). Application of GIS-Based AHP Model for the Impact Assessment of COVID-19 Lockdown on Environment Quality: The Case of Kabul City, Afghanistan. *J. of the Indian Society of Remote Sensing*, 1-14.
- 4) Allafta, H., & Opp, C. (2021). GIS-based multi-criteria analysis for flood prone areas mapping in the trans-boundary Shatt Al-Arab basin, Iraq-Iran. *Geomatics, Natural Hazards and Risk*, **12**(1), 2087-2116. <https://doi.org/10.1080/19475705.2021.1955755>
- 5) Arab, T. N. (2022). Eastern Afghanistan province, thousands of homes destroyed. <https://www.newarab.com/news/flash-floods-kill-20-eastern-afghanistan-province>
- 6) Aribisala, O. D., Yum, S.-G., & Song, M.-S. (2022). Flood Damage Assessment: A Review of Micro scale Methodologies for Residential Buildings. *Sustainability*, **14**(21), 13817. <https://doi.org/10.3390/su142113817>
- 7) Arshad, A., Zhang, Z., & Dilawar, A. (2020). Mapping favorable groundwater potential recharge zones using a GIS-based analytical hierarchical process and probability frequency ratio model: A case study from an agro-urban region of Pakistan. *Geoscience Frontiers*, **11**(5), 1805-1819. <https://doi.org/10.1016/j.gsf.2019.12.013>
- 8) Cabrera, & Lee. (2019). Flood-Prone Area Assessment Using GIS-Based Multi-Criteria Analysis: A Case Study in Davao Oriental, Philippines. *Water*, **11**(11), 2203. <https://doi.org/10.3390/w11112203>
- 9) Chen, Y.-R., Yeh, C.-H., & Yu, B. (2011). Integrated application of the analytic hierarchy process and the geographic information system for flood risk assessment and flood plain management in Taiwan. *Natural Hazards*, **59**(3), 1261-1276. <https://doi.org/10.1007/s11069-011-9831-7>
- 10) D'Addabbo, A., Refice, A., & Pasquariello, G. (2018). Dafne: A Matlab toolbox for Bayesian multi-source remote sensing and ancillary data fusion, with application to flood mapping. *Computers & Geosciences*, **112**, 64-75.
- 11) Das, S. (2019). Geospatial mapping of flood susceptibility and hydro-geomorphic response to the floods in Ulhas basin, India. *Remote Sensing Applications: Society and Environment*, **14**, 60-74.
- 12) Desalegn, H., & Mulu, A. (2021). Flood vulnerability assessment using GIS at Fetam watershed, upper Abbay basin, Ethiopia. *Heliyon*, **7**(1), e05865.
- 13) Dilley, M. (2005). Natural disaster hotspots: a global risk analysis (Vol. 5). *World Bank Publications*.
- 14) Feizizadeh, B. (2013). Integrating GIS based fuzzy set theory in multicriteria evaluation methods for landslide susceptibility mapping. *Inter J. of Geoinformatics*.
- 15) Gerlitz, L., Steirou, E., & Merz, B. (2018). Variability of the cold season climate in Central Asia. Part I: weather types and their tropical and extra tropical drivers. *J. of climate*, **31**(18), 7185-7207.
- 16) Ghosh, S., Das, A., & Alamri, A. M. (2020). Impact of COVID-19 induced lockdown on environmental quality in four Indian megacities using land sat 8 OLI and TIRS-derived data and mamdani fuzzy logic modeling approach. *Sustainability*, **12**(13), 5464.
- 17) Hasanloo, M., Pahlavani, P., & Bigdeli, B. (2019). Flood Risk Zonation Using a Multi-Criteria Spatial Group Fuzzy-Ahp Decision Making and Fuzzy Overlay Analysis. *The International Archives of the Photogrammetry, Remote Sensing and Spatial Information Sciences*, XLII-4/W18, 455-460. <https://doi.org/10.5194/isprs-archives-XLII-4-W18-455-2019>
- 18) Jeyaseelan, A. (2003). Droughts & floods assessment and monitoring using remote sensing and GIS. *Satellite remote sensing and GIS applications in agricultural meteorology*, 291.
- 19) Kachouri, S., Achour, H., & Bouaziz, S. (2014). Soil erosion hazard mapping using Analytic Hierarchy Process and logistic regression: a case study of Haffouz watershed, central Tunisia. *Arabian J. of Geosciences*, **8**(6), 4257-4268. <https://doi.org/10.1007/s12517-014-1464-1>

- 20) Khan, S. I., Hong, Y., & Irwin, D. (2011). Satellite Remote Sensing and Hydrologic Modeling for Flood Inundation Mapping in Lake Victoria Basin: Implications for Hydrologic Prediction in Ungauged Basins. *IEEE Transactions on Geoscience and Remote Sensing*, **49**(1), 85-95. <https://doi.org/10.1109/tgrs.2010.2057513>
- 21) Le Bihan, G., Payraastre, O., & Pons, F. (2017). The challenge of forecasting impacts of flash floods: test of a simplified hydraulic approach and validation based on insurance claim data. *Hydrology and Earth System Sciences*, **21**(11), 5911-5928. <https://doi.org/10.5194/hess-21-5911-2017>
- 22) Mahmoud, S. H., & Gan, T. Y. (2018). Multi-criteria approach to develop flood susceptibility maps in arid regions of Middle East. *J. of Cleaner Production*, **196**, 216-229.
- 23) Nasimi, M. N., Sagin, J., & Wijesekera, N. (2020). Climate and Water Resources Variation in Afghanistan and the Need for Urgent Adaptation Measures. *Int. J. Food Sci. Agric*, **4**, 49-64.
- 24) Naulin, J.-P., Payraastre, O., & Gaume, E. (2013). Spatially distributed flood forecasting in flash flood prone areas: Application to road network supervision in Southern France. *J. of Hydrology*, **486**, 88-99.
- 25) Nur MNB, Rahim MA, and Rasheduzzaman M. (2021). Flood impacts analysis and mitigation approach towards community resiliency at Nageshwari upazila, Kurigram, *Asian J. Soc. Sci. Leg. Stud.*, **3**(5), 178-192. <https://doi.org/10.34104/ajssls.021.01780192>
- 26) Ouma, Y., & Tateishi, R. (2014). Urban Flood Vulnerability and Risk Mapping Using Integrated Multi-Parametric AHP and GIS: Methodological Overview and Case Study Assessment. *Water*, **6**(6), 1515-1545. <https://doi.org/10.3390/w6061515>
- 27) Rahman, M. R. (2006). Flood inundation mapping and damage assessment using multi-temporal Radarsat and IRS 1C LISS III Image. *Asian J. of Geoinformatics*, **6**(2), 11-21.
- 28) Razandi, Y., Pourghasemi, H. R., & Rahmati, O. (2015a). Application of analytical hierarchy process, frequency ratio, and certainty factor models for groundwater potential mapping using GIS. *Earth Science Informatics*, **8**(4), 867-883.
- 29) Razandi, Y., Pourghasemi, H. R., & Rahmati, O. (2015b). Application of analytical hierarchy process, frequency ratio, and certainty factor models for groundwater potential mapping using GIS. *Earth Science Informatics*, **8**, 867-883.
- 30) Saaty, T. (1980). *The Analytic Hierarchy Process: Planning, Priority Setting, Resources Allocation*. McGraw-Hill, New York.
- 31) Saaty, T. L. (1977). A scaling method for priorities in hierarchical structures. *J. of mathematical psychology*, **15**(3), 234-281.
- 32) Saaty, T. L. (1990). An exposition of the AHP in reply to the paper "remarks on the analytic hierarchy process". *Management science*, **36**(3), 259-268.
- 33) Saaty, T. L., & Vargas, L. G. (2001). How to make a decision. In *Models, methods, concepts & applications of the analytic hierarchy process* (pp. 1-25). Springer.
- 34) Saha, A. K., & Agrawal, S. (2020). Mapping and assessment of flood risk in Prayagraj district, India: a GIS and remote sensing study. *Nanotechnology for Environmental Engineering*, **5**(2). <https://doi.org/10.1007/s41204-020-00073-1>
- 35) Sahak, A. S., Karsli, F., & Ahmadi, K. (2023). Seasonal monitoring of urban heat island based on the relationship between land surface temperature and land use/cover: a case study of Kabul City, Afghanistan. *Earth Science Informatics*, **16**(1), 845-861.
- 36) Seejata, K., Yodying, A., & Tantanee, S. (2018). Assessment of flood hazard areas using analytical hierarchy process over the Lower Yom Basin, Sukhothai Province. *Procedia engineering*, **212**, 340-347.
- 37) Şener, E., Şener, Ş., & Davraz, A. (2018a). Groundwater potential mapping by combining fuzzy-analytic hierarchy process and GIS in Beyşehir Lake Basin, Turkey. *Arabian J. of Geosciences*, **11**(8), 1-21.
- 38) Şener, E., Şener, Ş., & Davraz, A. (2018b). Groundwater potential mapping by combining fuzzy-analytic hierarchy process and GIS in Beyşehir Lake Basin, Turkey. *Arabian J. of Geosciences*, **11**, 1-21.

- 39) Stefanidis, S., & Stathis, D. (2013). Assessment of flood hazard based on natural and anthropogenic factors using analytic hierarchy process (AHP). *Natural Hazards*, **68**(2), 569-585. <https://doi.org/10.1007/s11069-013-0639-5>
- 40) Tang, Z., Zhang, H., & Xiao, Y. (2018). Assessment of flood susceptible areas using spatially explicit, probabilistic multi-criteria decision analysis. *J. of Hydrology*, **558**, 144-158.
- 41) Tavus, B., Kocaman, S., & Gokceoglu, C. (2022). Flood damage assessment with Sentinel-1 and Sentinel-2 data after Sardoba dam break with GLCM features and Random Forest method. *Science of the Total Environment*, **816**, 151585.
- 42) Veljanovski, T., Lamovec, P., and Oštir, K. (2011). Comparison of three techniques for detection of flooded areas on ENVISAT and RADARSAT-2 satellite images. *V: Geoinformation for disaster management*, Gi4DM.
- 43) Vu, T. T., Nguyen, P. K., & Law, A. W. (2015). Two-dimensional hydrodynamic modelling of flood inundation for a part of the Mekong River with TELEMAC-2D. *British J. of Environment and Climate Change*, **5**(2), 162-175.
- 44) Wang, Y., Li, Z., & Zeng, G. (2011). A GIS-Based Spatial Multi-Criteria Approach for Flood Risk Assessment in the Dongting Lake Region, Hunan, Central China. *Water Resources Management*, **25**(13), 3465-3484. <https://doi.org/10.1007/s11269-011-9866-2>
- 45) Yahaya, S., Ahmad, N., & Abdalla, R. F. (2010). Multicriteria analysis for flood vulnerable areas in Hadejia - Jama'are River basin, Nigeria. *European J. of Scientific Research*, **42**(1), 71-83.
- 46) Zhang, J., & Chen, Y. (2019). Risk Assessment of Flood Disaster Induced by Typhoon Rainstorms in Guangdong Province, China. *Sustainability*, **11**(10), 2738. <https://doi.org/10.3390/su11102738>

Citation: Ahmadi K, Sahak AS, Azizi AB, Saraj MA, and Sahak AT. (2024). Analyzing flood damage and mapping flood hazard zones using AHP model: a case study of Pol-e-Alam, Logar province, Afghanistan. *Aust. J. Eng. Innov. Technol.*, **6**(2), 37-50. <https://doi.org/10.34104/ajeit.024.037050> 